Lawrence Berkeley National Laboratory
Recent Work

Title
THERMAL-EXPANSION INDUCED CELLULAR FLAMES

Permalink
https://escholarship.org/uc/item/6xr69989

Authors
Michelson, D.M.
Sivashinsky, G.I.

Publication Date
1982-03-01

eScholarship.org Powered by the California Digital Library
University of California

LBL-14217
Preprint

Lawrence Berkeley Laboratory
UNIVERSITY OF CALIFORNIA

Physics, Computer Science & Mathematics Division

RECEIVED
LAWRENCE
BERKELEY LABORATORY
JUN 2 1982
LIBRARY AND
DOCUMENTS SECTION

To be submitted for publication

THERMAL-EXPANSION INDUCED CELLULAR FLAMES

D.M. Michelson and G.I. Sivashinsky

March 1982

TWO-WEEK LOAN COPY

This is a Library Circulating Copy which may be borrowed for two weeks. For a personal retention copy, call Tech. Info. Division, Ext. 6782.

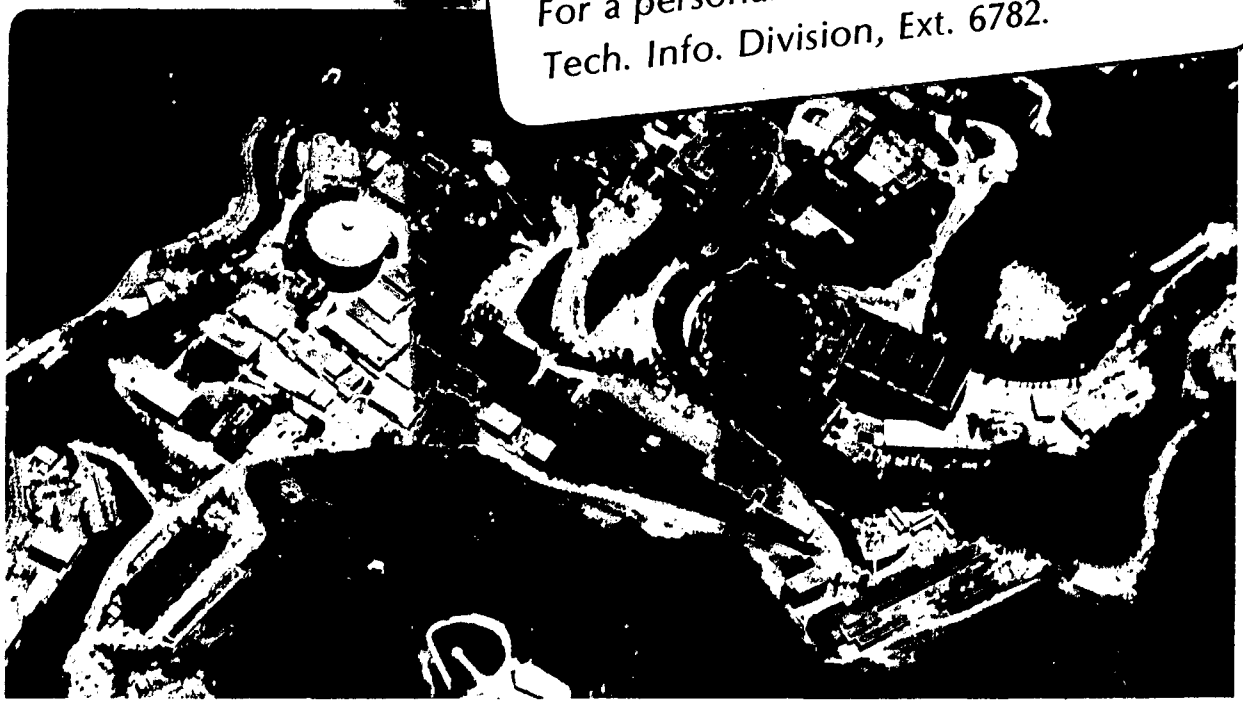

Prepared for the U.S. Department of Energy under Contract DE-AC03-76SF00098

LBL-14217

DISCLAIMER

This document was prepared as an account of work sponsored by the United States Government. While this document is believed to contain correct information, neither the United States Government nor any agency thereof, nor the Regents of the University of California, nor any of their employees, makes any warranty, express or implied, or assumes any legal responsibility for the accuracy, completeness, or usefulness of any information, apparatus, product, or process disclosed, or represents that its use would not infringe privately owned rights. Reference herein to any specific commercial product, process, or service by its trade name, trademark, manufacturer, or otherwise, does not necessarily constitute or imply its endorsement, recommendation, or favoring by the United States Government or any agency thereof, or the Regents of the University of California. The views and opinions of authors expressed herein do not necessarily state or reflect those of the United States Government or any agency thereof or the Regents of the University of California.

LBL-14217

THERMAL-EXPANSION INDUCED CELLULAR FLAMES[1]

D.M. Michelson

Department of Mathematics
University of California
Los Angeles, California 90024

G.I. Sivashinsky[2]

Department of Mathematics and Lawrence Berkeley Laboratory
University of California
Berkeley, California 94720

March 1982

[1]This work was supported in part by the Director, Office of Energy Research, Office of Basic Energy Sciences, Engineering, Mathematical, and Geosciences Division of the U.S. Department of Energy under contract DE-AC03-76SF00098.

[2]On leave from the Department of Mathematical Sciences, Tel-Aviv University, Ramat-Aviv, P.O.B. 39040, Tel-Aviv 69978, Israel.

This manuscript was printed from originals provided by the authors.

THERMAL-EXPANSION INDUCED CELLULAR FLAMES

D.M. Michelson

Department of Mathematics
University of California
Los Angeles, California 90024

G.I. Sivashinsky

Department of Mathematics and Lawrence Berkeley Laboratory
University of California
Berkeley, California 94720

Abstract

This paper is devoted to a study of the nonlinear evolution of a disturbed plane flame front in a hydrodynamic instability regime induced by thermal expansion of the burnt gas.

It is shown that, in sufficiently small-scale flames, spontaneous instability appears in the guise of stationary wide-spaced irregular folds. However, in sufficiently large-scale flames, one encounters a completely new type of hydrodynamic instability: the flame front splits into separate cells which are constantly subdividing and merging in a *chaotic* manner. The average dimension of the cells is approximately five times greater than the wavelength of the disturbance which has the highest amplification rate (according to the linear theory).

1. Introduction

In a recent paper on hydrodynamic instability of premixed flames [1] the following equation describing the evolution of the perturbed flame front was derived

$$F_t + \tfrac{1}{2} U_b (\nabla F)^2 = D_{th}[1 + \tfrac{1}{2}\beta(Le-1)]\nabla^2 F + \tfrac{1}{2} U_b (1-\varepsilon) I\{F\} \qquad (1)$$

where

$$I\{F\} = \frac{1}{4\pi^2} \int_{-\infty}^{\infty} |\vec{k}| e^{i\vec{k}(\vec{x}-\vec{x}')} F(\vec{x}',t) d\vec{k} d\vec{x}' .$$

Here $z = F(x,y,t)$ is a perturbation of a plane flame front; U_b is the velocity of the undisturbed plane flame front relation to the burnt gas; D_{th} is the thermal diffusivity of the gas, $Le = D_{th}/D_{mol}$ - Lewis number; D_{mol} is the diffusivity of the deficient reactant; $\beta = E(T_b - T_u)/R^0 T_b^2$, where T_u, T_b are the temperatures of the unburnt and burnt gas, respectively; E is the activation energy; R^0 is the universal gas constant; $\varepsilon = \rho_u/\rho_b$ is the density ratio (thermal expansion coefficient); $l_{th} = D_{th}/U_b$ is the flame thickness. Eq. (1) was derived on the assumption that the thermal expansion of the gas is weak, i.e. $(1-\varepsilon) \ll 1$.

It is readily seen that the dispersion relation corresponding to the linear stability problem for a plane flame front ($F \equiv 0$) is

$$\sigma = \tfrac{1}{2}(1-\varepsilon) U_b k - [1 + \tfrac{1}{2}\beta(Le-1)] D_{th} k^2 \qquad (2)$$

$$(F \sim \exp(\sigma t + i\vec{k}\vec{x}) \ , \ k = |\vec{k}|) .$$

Hence it follows that if $Le > Le_c = 1 - 2/\beta$ (i.e., in the absence of thermo-diffusive instability [1]) there exists a wavelength $\lambda_c = 2\pi/k_c$ corresponding to the maximum amplification rate o small disturbances (maximum σ).

Contrary to this prediction of the linear analysis, numerical experiments with the one-dimensional version of Eq. (1) in an interval of width $10\lambda_c$ showed that during the flame's nonlinear evolution there develop only one or two steady folds, showing very sharp edges toward the burned gas [2] (Fig. 1). The speed of the wrinkled flame

$U_w = U_b - F_t$ is almost independent of the initial disturbance; it is approximately:

$$U_w = U_b[1+0.18(1-\varepsilon)^2] .$$

Numerical experiments with Eq. (1) are conveniently done after writing it in the following parameter-free form, which is obtained by an elementary rescaling of the variables:

$$\Phi_\tau = \nabla^2\Phi - \tfrac{1}{2}(\nabla\Phi)^2 + \tfrac{1}{2} I\{\Phi\} . \qquad (3)$$

The shape of the steady-state front, i.e., the dimensions of the arc-shaped folds and their distribution over the front, depends essentially on the initial disturbance. The distance between adjacent folds may be significantly greater than the wavelength $\lambda_c = 2\pi/k_c$ corresponding to the highest amplification rate of small disturbances (according to the linear theory).[3] Such folds are frequently formed when the flame crosses various kinds of obstacles, such as electrodes [4] or a widely-spaced wire grid [3].

The effects of diffusion and head conduction are obviously most significant in the zone of the cusp, where the curvature of the front is extremely large. Outside this region the flame may be described perfectly well by the following truncated equation, corresponding to the Darrieus-Landau model:

$$F_t + \tfrac{1}{2} U_b(\nabla F)^2 = \tfrac{1}{2}(1-\varepsilon) U_b I\{F\} . \qquad (4)$$

Since the Darrieus-Landau model does not involve any characteristic length, Eq. (4) permits the existence of flames in which the distances between consecutive folds are arbitrarily large.

If the distance between the folds is increased indefinitely, the stabilizing effects of stretching and curvature are weakened, and one expects new folds to appear. Thus, in order to investigate the fully developed hydrodyanamic instability one must consider sufficiently large-scale flames. Experiments of this type were recently carried out, in

[3]Eq. (1) provides an example of how the characteristic structure dimension $(2\pi/k_c)$ predicted by linear stability analysis may differ significantly from the dimension yielded by the original nonlinear system.

connection with the investigation of accidental industrial explosions, by Lind and Whitson [5] and Ivashchenko and Rumiantsev [6]. Lind and Whitson experimented with lean hydrocarbon-air mixtures in 0.05 mm thick polyethylene film hemispheres of 5 m and 10 m radius. Ivashchenko and Rumiantsev carried out similar experiments in 0.05 to 0.08 mm thick rubber spherical shells of 2.5 m radius. It was noticed that, as the flame expanded, it became rough, with a "pebbled" appearance. This structure increased in size to about 0.4 to 1.0 m, with *finer* structure superimposed. It was observed that for systems with markedly different burning velocities the measured space velocity was 1.6 to 1.8 times the expected value, calculated from the normal burning velocity measured in the laboratory (Lind & Whitson [5]).

Ivashchenko and Rumiantsev also noted that when the sphere radius reached ~5 cm the flame became cellular, with cells about 1 to 2 cm in size. As the flame sphere grew the cell size increased, reaching ~6 to 10 cm for sphere radius ~0.3 to 0.5 m. As the cells appeared the flame propagation speed increased, reaching its maximum value at radius ~0.3 to 0.5 m. The maximum speed was 1.5 to 2 times the speed of the undisturbed spherical flame.

Of the earlier experimental observations of hydrodynamic instability in flames, we would like to mention the work of Simon and Wong [7], studying flames in a rich methane-air mixture filling a soap bubble of initial radius ~5 cm. When the flame radius was ~1.5 cm, the initially smooth flame front took on a cellular appearance, and simultaneously the flame was seen to accelerate. However, the relatively small volume of the mixture did not permit a sufficiently developed cellular instability and the wrinkled flame did not reach the uniform propagation mode.

2. **Two-dimensional patterns.**

It turns out that the nonlinear equation (1), considered in a sufficiently wide region, may describe (in addition to the wide-spaced folds) also cellular instability of the flame.

Fig. 2 shows the results of a numerical solution of the one-dimensional version of Eq. (1) over interval of length $40\lambda_c$ with periodic boundary conditions. As we see, in this case irregularity fluctuating cells do indeed appear together with the large-scale substructure (one fold).

The average cell dimension is about 5 times greater than the characteristic wavelength λ_c predicted by linear stability analysis. For example, taking $\varepsilon = 0.2$, $\beta = 15$, $Le = 1.2$, $l_{th} = 0.02$ cm the average cell dimension ($5\lambda_c$) is approximately 7.5 cm. This estimate is in reasonable agreement with experimental observations. The average propagation velocity of the flame is $U_w = U_b[1+0.4(1-\varepsilon)^2]$ which is markedly greater than that obtained for an interval of length $10\lambda_c$, when cellular structure does not develop at all.

3. **Three-dimensional patterns**

One can best understand the nature of hydrodynamic instability by considering the two-dimensional version of Eq. (1), which describes the evolution of the actual flame *surface*.

Fig. 3 presents the results of solving Eq. (1) in a square $5\lambda_c \times 5\lambda_c$ with periodic boundary conditions.[4] As initial disturbance we took the function

$$F(x,y,0) = 4l_{th}\cos(k_c x)\cos(k_c y)\,. \qquad (5)$$

The limiting steady configuration is in good agreement with studies of the one-

[4]The new numerical computation method used here is described in the Appendix.

dimensional problem (Fig. 1) and also with experimental observations [3,4].

In this case the propagation speed of the wrinkled flame is $U_w = U_b[1+0.3(1-\varepsilon)^2]$, i.e., appreciably higher than in the one-dimensional case (Fig. 1).

However, in order to observe cellular instability one must enlarge the domain so much as to require an enormous amount of computer time. Fortunately, this difficulty can be avoided. Recall that in an expanding spherical flame the cell size at the stability threshold is considerably less than that reached in flame propagation. A similar cell-diminishing effect may be obtained by considering a spherical flame stabilized on a point source of combustible mixture or a plane flame in a stabilizing acceleration field. Conditions resembling the last-named case are observed in a flame in a periodically varying acceleration field [3].

Thus, if one introduces such effects as stretching, curvature or acceleration, cells may be observed even in a $5\lambda_c \times 5\lambda_c$ square. For example, to incorporate the effect of curvature, it suffices to augment the right-hand side of Eq. (1) by the term $-(2U_b/R)F$, where R is the radius of the undisturbed flame [8].

With curvature included, the dispersion relation (2) is modified, to become:

$$\sigma = \tfrac{1}{2}(1-\varepsilon)U_b k - [1+\tfrac{1}{2}\beta(Le-1)]D_{th}k^2 - (2U_b/R)\,. \qquad (6)$$

Hence, when the flame radius falls below a certain critical value R_c, σ is negative for all k. Thus a spherical flame of sufficiently small radius is stable, instability setting in at $R > R_c$. Near the stability threshold the unstable modes concentrate around λ_c – the wavelength corresponding to maximum amplification rate σ.

Fig. 4 shows the result of a numerical solution of the initial-value problem for the case $R = 1.2R_c$. The domain, boundary conditions and initial data are identical to those employed in the preceding case (Fig. 3). Now, however, the flame front ultimately takes the form of a stationary regular hexagonal cellular structure.[5] The cell

[5]When R is near R_c this structure may also be constructed analytically, using a familiar technique of bifurcation theory (e.g. [8]).

size is determined by the critical wavelength λ_c.

Let us see what happens when the flame radius R is increased. Fig. 5 illustrates the successive evolution of the flame front at $R = 6.25R_c$ and initial data (5). At first, the flame front assumes a quasi-regular hexagonal structure. However, this stage is now transient. With the passage of time, the quasi-regular arrangement of cells disappears, their average diameter constantly increases and reaches the order of $3\lambda_c$. It is interesting to note that the general configuration of the flame front shows no tendency to stabilize. The cells are in a state of permanent irregular recombination. Although the smallness of the domain and the curvature effect influence the behavior of the disturbed flame, the resulting configuration as a whole is in qualitative agreement with the results of the one-dimensional analysis (Fig. 2).

4. **Concluding remarks**

Our numerical experiments suggest that in large-scale flames heat-expansion induced instability may appear in two guises:

(i) deep folds, actually described by the truncated Eq. (4) and therefore having no characteristic size;

(ii) fine structure (cells) of a characteristic size depending on diffusion effects.

In relatively small-scale flames, it is fairly difficult to introduce a reasonable definition that makes a distinction between the two patterns. However, observations of expanding spherical flames indicate that the disturbances formed at the initial stage of flame propagation are representatives of the type (i) pattern.

Numerical experiments show that an increase in flame aspect ratio implies an increase in propagation speed. However, stabilization of the velocity of a cellular flame is a slow process, and as yet we have not been able to determine the limiting value of the average velocity corresponding to an "infinite" plane self-turbulent flame. On the

other hand, the slow stabilization of the velocity is in good agreement with experimental data [4,6].

In the case of lean methane-air mixtures, hydrodynamic instability should combine with thermo-diffusive instability, which may appear as small cells superimposed on the larger heat-expansion induced cells. However, there is no mention of this effect in [6]. Perhaps the superfine structure was too weakly expressed to be easily detected.

In conclusion, we would like to point out other possible influences, such as effects of steady or time-varying acceleration (Taylor instability, interaction of pressure waves with the flame), that may cause small-scale cellular structure [3].

Acknowledgments

The authors are indebted to Professor F.A. Williams for the information he kindly provided concerning the work of Lind and Whitson. During the course of this research D.M. Michelson was supported by National Science Foundation Grant MCS78-01252, while G.I.Sivashinsky was jointly supported by the Israel Commission for Basic Research, by U.S.-Israel Binational Science Foundation and by the Director, Office of Energy Research, Office of Basic Energy Sciences, Engineering, Mathematical, and Geosciences Division of the U.S. Department of Energy, under contract DE-AC03-76SF00098.

APPENDIX

In the two-dimensional case, Eq. (3) was solved in the region $-l \le \xi, \eta \le l, \tau \ge 0$ with initial conditions $\Phi(\xi,\eta,0) = \Phi_0(\xi,\eta)$, and periodic boundary conditions. In view of the boundary conditions, the function Φ and the integral operator $I\{\Phi\}$ may be expressed as follows:

$$\Phi(\xi,\eta,\tau) = \sum_{m,n=-\infty}^{\infty} a_{mn}(\tau) e^{\frac{i\pi}{l}(m\xi+n\eta)} \tag{A1}$$

$$I\{\Phi\} = \sum_{m,n=-\infty}^{\infty} \frac{\pi}{l}\sqrt{m^2+n^2}\, a_{mn}(\tau) e^{\frac{i\pi}{l}(m\xi+n\eta)} . \tag{A2}$$

We now define mesh points (ξ_i,η_j,τ_k) in the region in which the equation is to be solved:

$$\xi_i = -l+i\Delta\xi \ , \ n_j = -l+j\Delta\eta \ , \ \tau_k = k\Delta\tau \tag{A3}$$

where $0 \le i, j \le N-1$, $\Delta\xi = \Delta\eta = 2l/N$. The values of the function $\Phi(\xi,\eta,\tau)$ at the mesh points are denoted by

$$\Phi(\xi_i,\eta_j,\tau_k) = \Phi^k_{i,j} . \tag{A4}$$

Eq. (3) will be solved by the so-called splitting method. That is, we express Eq. (3) as

$$\Phi_\tau = L_1\Phi + L_2\Phi \tag{A5}$$

where

$$L_1\Phi \equiv \nabla^2\Phi + \tfrac{1}{2} I\{\Phi\} \ , \ L_2\Phi \equiv -\tfrac{1}{2}(\nabla\Phi)^2 .$$

The nonlinear term $L_2\Phi$ is split into a sum

$$L_2\Phi = L_{2,\xi}\Phi + L_{2,\eta}\Phi \equiv -\tfrac{1}{2}\Phi_\xi^2 - \tfrac{1}{2}\Phi_\eta^2 . \tag{A6}$$

Suppose we know the value of $\Phi(\xi,\eta,\tau)$ at time $\tau = \tau_0$. The following three problems may be associated with Eq. (A5):

$$\Phi^{(1)}_\tau = L_1\Phi^{(1)} \ , \ \tau_0 \le \tau \le \tau_0 + \Delta\tau \ , \ \Phi^{(1)}(\xi,\eta,\tau_0) = \Phi(\xi,\eta,\tau_0) , \tag{A7}$$

$$\Phi_\tau^{(2)} = L_{2,\xi}\Phi^{(2)} \ , \ \tau_0 \le \tau \le \tau_0 + \Delta\tau \ , \ \Phi^{(2)}(\xi,\eta,\tau_0) = \Phi^{(1)}(\xi,\eta,\tau_0+\Delta\tau) \ . \qquad \textbf{(A8)}$$

$$\Phi_\tau^{(2)} = L_{2,\eta}\Phi^{(3)} \ , \ \tau_0 \le \tau \le \tau_0 + \Delta\tau \ , \ \Phi^{(3)}(\xi,\eta,\tau_0) = \Phi^{(2)}(\xi,\eta,\tau_0+\Delta\tau) \ . \qquad \text{(A9)}$$

The function $\Phi^{(3)}(\xi,\eta,\tau_0+\Delta\tau)$ approximates the exact solution $\Phi(\xi,\eta,\tau_0+\Delta\tau)$ of Eq. (A5) to within $0((\Delta\tau)^2)$, i.e.,

$$\Phi(\xi,\eta,\tau_0+\Delta\tau) = \Phi^{(3)}(\xi,\eta,\tau_0+\Delta\tau) + 0((\Delta\tau)^2) \ . \qquad \text{(A10)}$$

Since Eq. (A7) is linear with constant coefficients and periodic boundary conditions, it is natural to solve it by Fourier methods. The discrete analog of the Fourier series (A1) is

$$\Phi(\xi,\eta,\tau) = \sum_{m,n=-N/2}^{N/2} a_{mn}(\tau) e^{\frac{i\pi}{l}(m\xi+n\eta)} \qquad \text{(A11)}$$

where $(\xi,\eta) = (\xi_i,\eta_j)$. The coefficients $a_{mn}(\tau_0)$ may be derived from the function values $\Phi(\xi_i,\eta_j,\tau_0)$ by fast Fourier transform. We then obtain from (A7)

$$a_{mn}(\tau_0+\Delta\tau) = \exp[(-\gamma_{mn}^2 + \tfrac{1}{2}\gamma_{mn})\Delta\tau] a_{mn}(\tau_0) \qquad \text{(A12)}$$

where $\gamma_{mn} = (\pi/l)\sqrt{m^2+n^2}$. Once we know $a_{mn}(\tau_0+\Delta\tau)$, we can determine $\Phi^{(1)}(\xi_i,\eta_j,\eta_0+\Delta\tau)$ using Eq. (A12) and the fast Fourier transform.

Problems (A8) and (A9) are solved by finite differences. Note that in the solution of problem (A7) the stability condition imposes no restrictions on the spacing $\Delta\tau$. In order to maintain $\Delta\tau$ as large as possible, the following implicit scheme was used to solve Eq. (A8):

$$\frac{\Phi_{ij}^1 - \Phi_{ij}^0}{\Delta\tau} = -\frac{1}{4}\left[\left(\frac{\partial\Phi}{\partial\xi}\right)_{ij}^1 \frac{\Phi_{i+1,j}^0 - \Phi_{i-1,j}^0}{2\Delta\xi} + \left[\frac{\Phi_{i+1,j}^0 - \Phi_{i-1,j}^0}{2\Delta\xi}\right]^2\right] . \qquad \text{(A13)}$$

The superscript 0 or 1 in this formula indicates that the function is computed at time τ_0 or $\tau_0+\Delta\tau$, respectively. The coefficients are found from (A8) using the explicit scheme of the first-order accuracy

$$\left[\frac{\partial\Phi}{\partial\xi}\right]^1_{ij} = \frac{\Phi^0_{i+1,j}-\Phi^0_{i-1,j}}{2\Delta\xi}\left[1 - \frac{\Delta\tau}{(\Delta\xi)^2}\left(\Phi^0_{i+1,j} - 2\Phi^0_{i,j} + \Phi^0_{i-1,j}\right)\right]. \qquad \textbf{(A14)}$$

Together with periodic boundary conditions, Eq. (A13) yields a system of linear equations for the unknown functions Φ^1_{ij}. The coefficient matrix of this system is 3-diagonal and is therefore easily inverted. Eq. (A9) is solved by the same method.

The linear stability analysis imposes no restrictions on the spacings $\Delta\xi,\Delta\eta,\Delta\tau$. The optimum spacings were therefore determined experimentally. The spacing $\Delta\xi$ may be estimated roughly, based on the reasoning that the critical wavelength 8π should contain ~10 intervals $\Delta\xi$. In the solution of the two-dimensional problem we took $\Delta\xi = \Delta\eta = \Delta\tau = 2$ and $N = 64$ (number of mesh points). Choosing N as a power of 2 guaranteed maximum efficiency of the fast Fourier transform. Thus, an interval of length $2l = N\Delta\xi$ included approximately 5 critical wavelengths. The computation rate (CPU) was approximately 1 minute per 60 time steps. In each case the solution was continued until the flame had settled down to a steady or pulsating regime; this required some 250 time steps.

REFERENCES

1. Sivashinsky, G.I., Nonlinear analysis of hydrodynamic instability in laminar flames. Part I. Derivation of basic equations. *Acta Astronautica* 4(11-12):1177-1206 (1977).

2. Michelson, D.M., and Sivashinsky, G.I., Nonlinear analysis of hydrodynamic instability in laminar flames. Part II. Numerical experiments. *Acta Astronautica* 4(11-12):1207-1221 (1977).

3. Markstein, G.H., *Nonsteady Flame Propagation*, Pergamon Press, Oxford, 1964.

4. Palm-Leis, A., and Strehlow, R.A., On the propagation of turbulent flames. *Combust. Flame* 13:111-129 (1969).

5. Lind, C.D., and Whitson, J., Explosion hazards associated with spills of large quantities of hazardous materials. Phase II. Report #CG-D-85-77. Dept. of Transportation, U.S. Coast Guard Report ADA-04758 (1977).

6. Ivashchenko, P.F., Rumiantsev, V.S., Convective rise and propagation velocity of a large flame focus. *Fiz. Gorenia Vzryva* 40:83-87 (1978).

7. Simon, D.M., and Wong, E.L., Burning velocity measurement. *J. Chem. Phys.* 21:936 (1953).

8. Sivashinsky, G.I., On self-turbulization of a laminar flame. *Acta Astronautica* 6:569-591 (1979).

FIGURE CAPTIONS

Fig. 1. Downward-propagating stationary folded flame front. Each curve represents the configuration of the flame front at four consecutive equidistant instants of time. Runs (a) and (b) correspond to different initial disturbances.

Fig. 2. Downward-propagating flame front in cellular instability regime.

Fig. 3. Downward-propagating stationary flame front with four folds. Three-dimensional pattern.

Fig. 4. Stationary flame front with regular hexagonal cells at $R = 1.2R_c$. Three-dimensional pattern.

Fig. 5. Successive evolution of flame front at $R = 6.25R_c$. Configurations (a)(b)(c)(d) correspond to times $\tau = 120, 360, 720, 1040$.

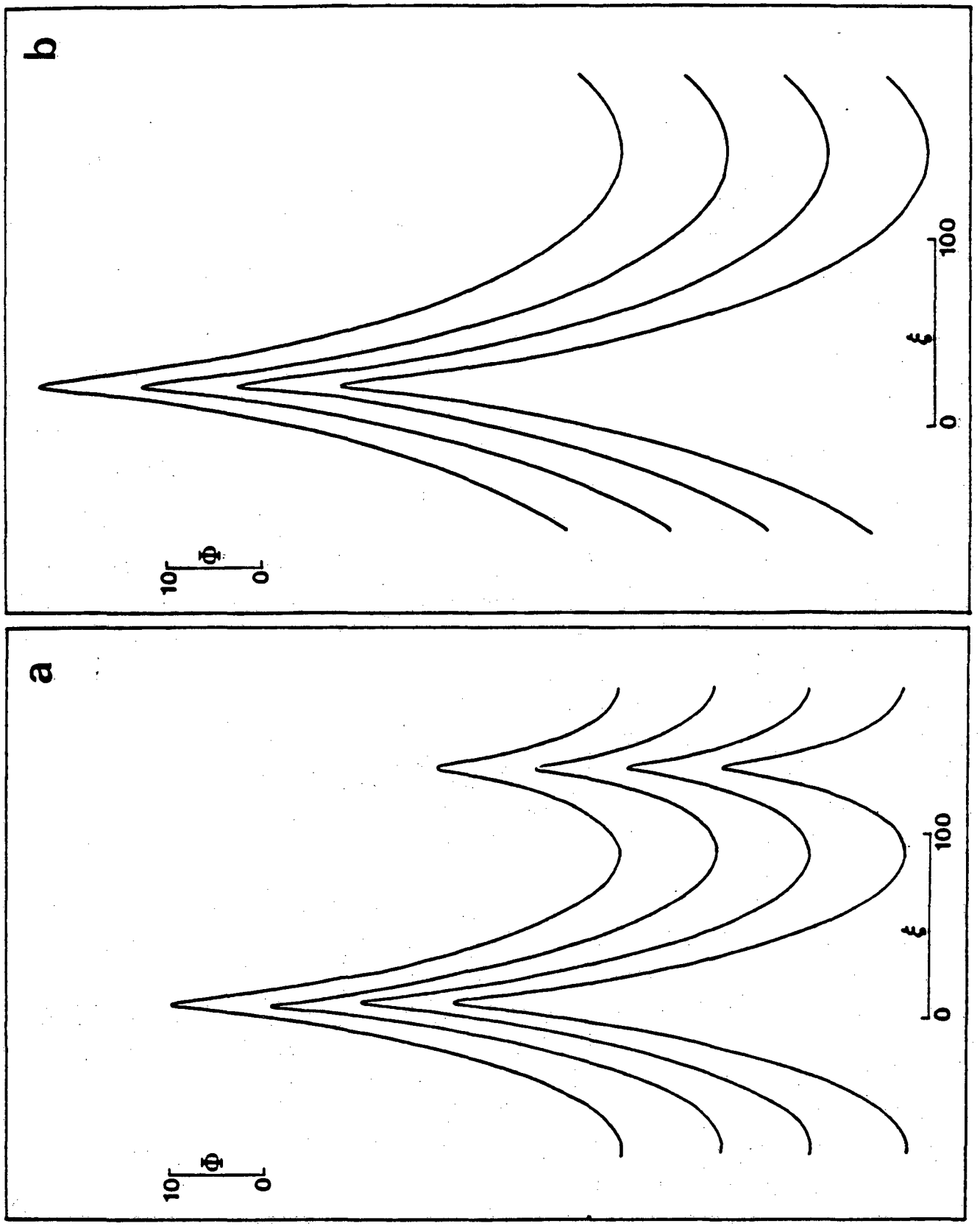

Figure 1

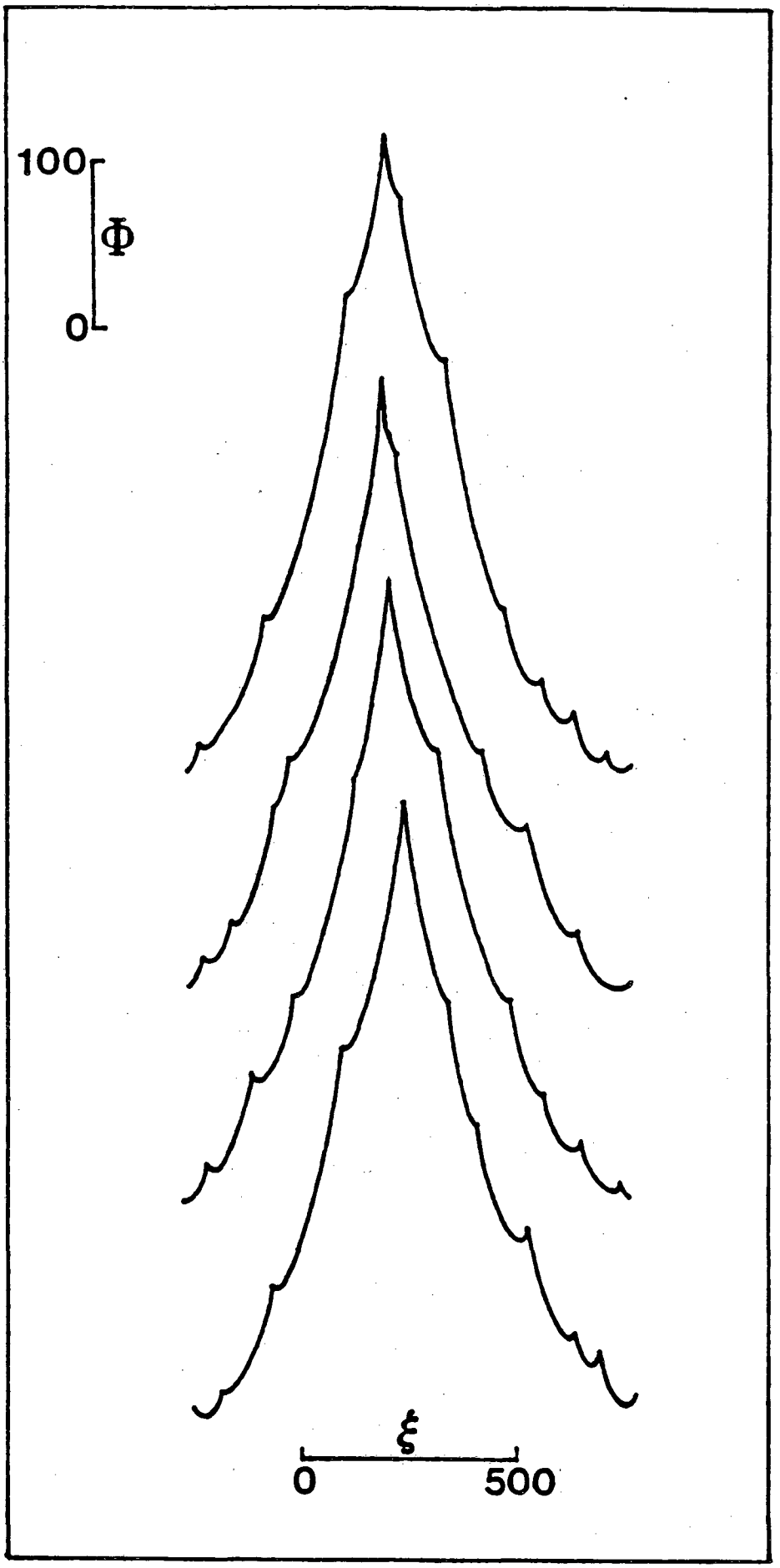

Figure 2

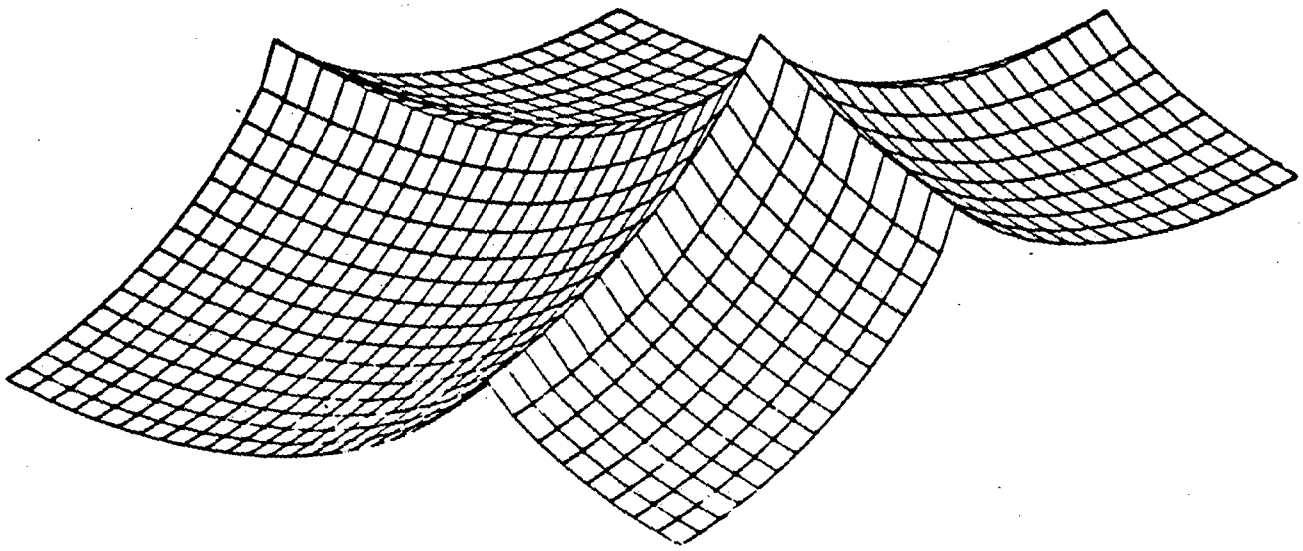

Figure 3

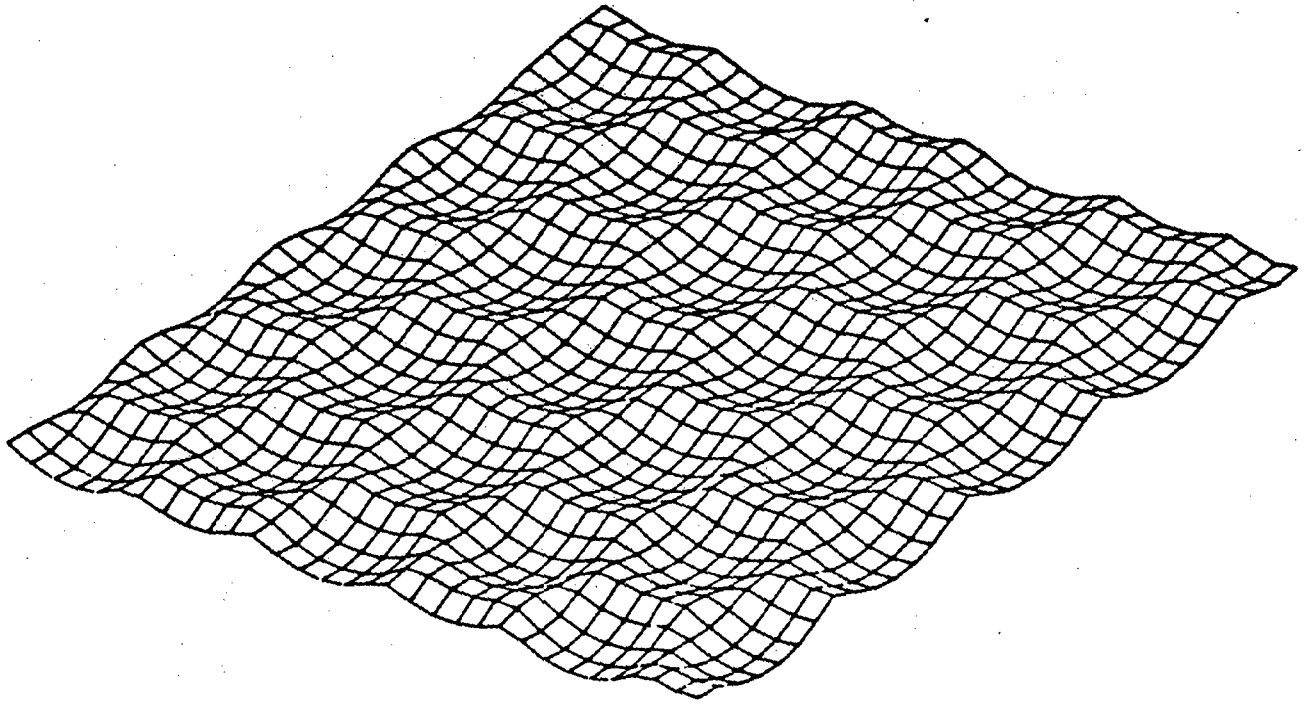

Figure 4

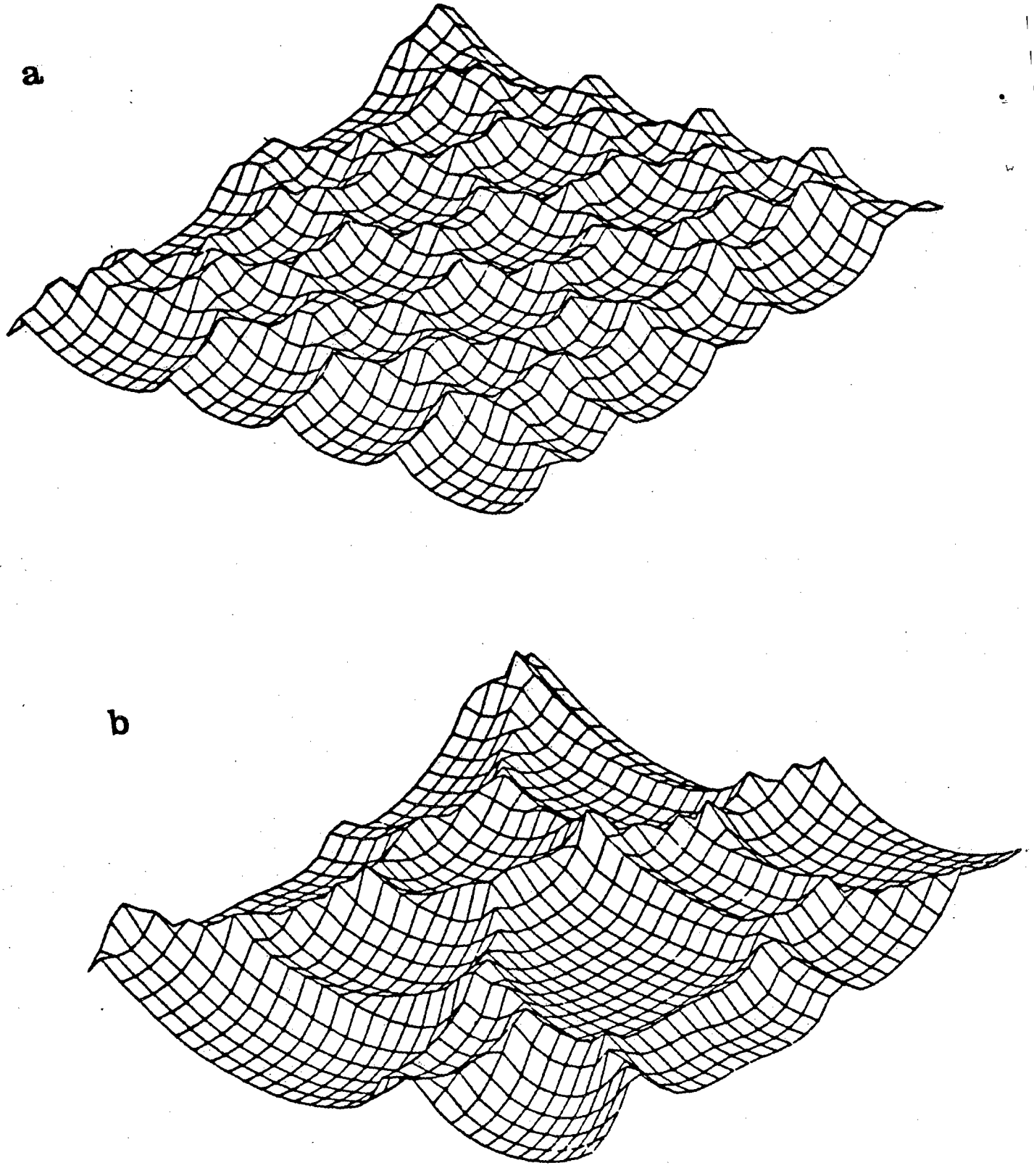

Figure 5 (a,b)

c

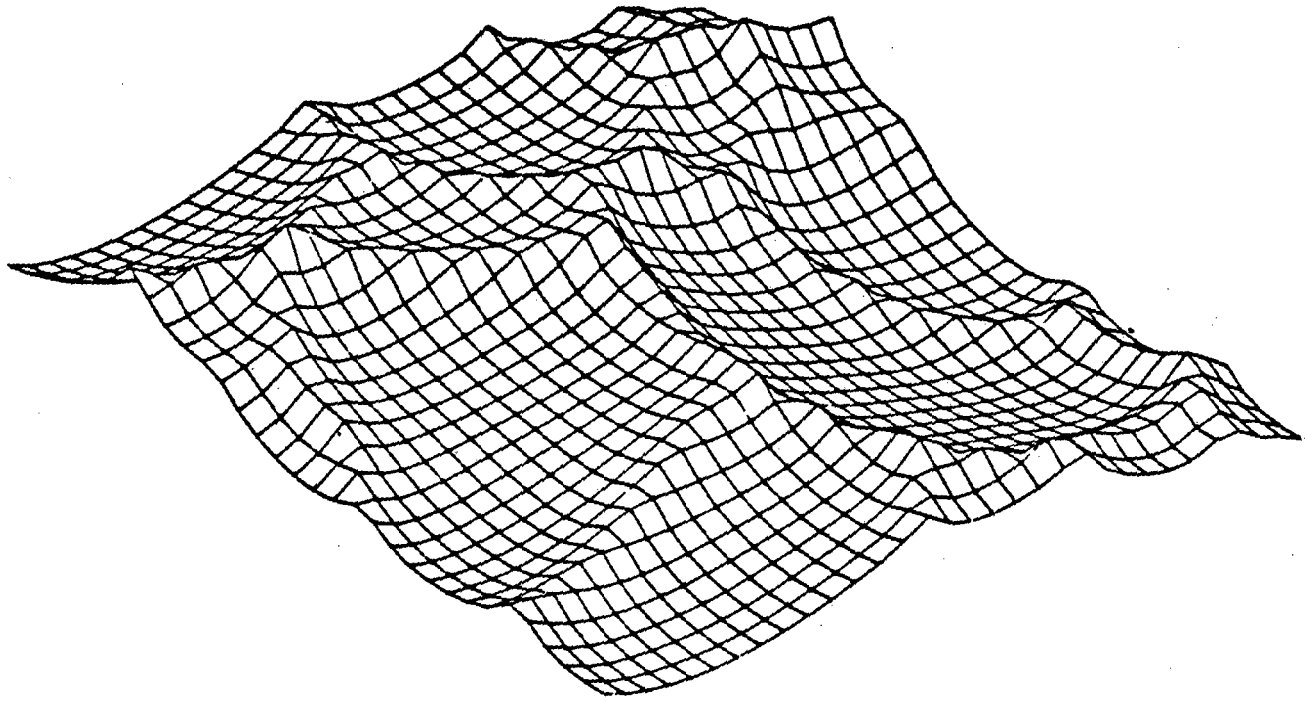

d

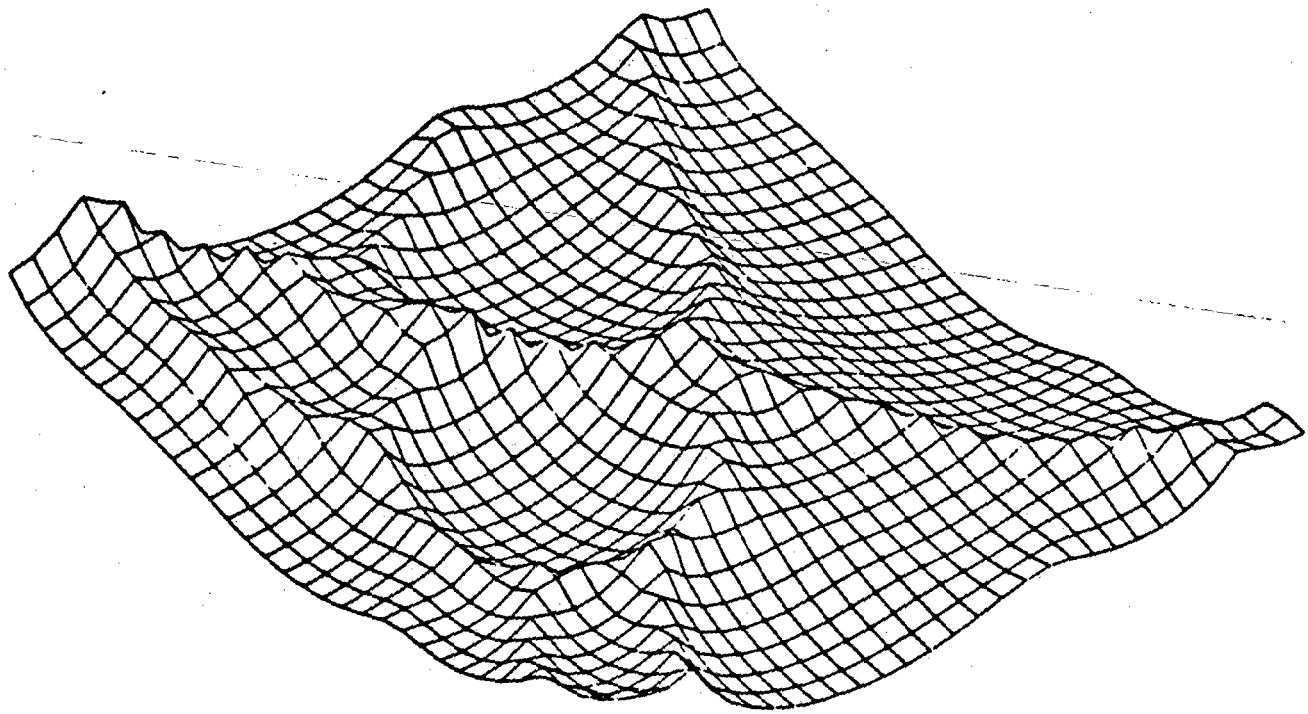

Figure 5 (c,d)

This report was done with support from the Department of Energy. Any conclusions or opinions expressed in this report represent solely those of the author(s) and not necessarily those of The Regents of the University of California, the Lawrence Berkeley Laboratory or the Department of Energy.

Reference to a company or product name does not imply approval or recommendation of the product by the University of California or the U.S. Department of Energy to the exclusion of others that may be suitable.

TECHNICAL INFORMATION DEPARTMENT
LAWRENCE BERKELEY LABORATORY
UNIVERSITY OF CALIFORNIA
BERKELEY, CALIFORNIA 94720